Nuclear Engineering and Technology 55 (2023) 1871–1877

Contents lists available at ScienceDirect

Nuclear Engineering and Technology

journal homepage: www.elsevier.com/locate/net

Original Article

Nano Yttrium-90 and Rhenium-188 production through medium medical cyclotron and research reactor for therapeutic usages: A Simulation study

Abdollah Khorshidi [a, b]

[a] School of Paramedical, Gerash University of Medical Sciences, Gerash, Iran
[b] Soleimani Maktab, Central Branch, Qaem University, Kerman, Iran

ARTICLE INFO

Article history:
Received 25 December 2022
Received in revised form
21 January 2023
Accepted 8 February 2023
Available online 14 February 2023

Keywords:
Medium reactor
Compact cyclotron
Neutron flux
Beta emitter
Neutron activator
Nano solution
Transmutation
Production yield
Specific activity

ABSTRACT

The main goal of the coordinated project development of therapeutic radiopharmaceuticals of Y-90 and Re-188 is to exploit advancements in radionuclide production technology. Here, direct and indirect production methods with medium reactor and cyclotron are compared to evaluate derived neutron flux and production yield. First, nano-sized ^{186}W and ^{89}Y specimens are suspended in water in a quartz vial by FLUKA simulation. Then, the solution is irradiated for 4 days under 9E+14 n/cm2/s neutron flux of reactor. Also, a neutron activator including three layers—lead moderator, graphite reflector, and polyethylene absorbent— is simulated and tungsten target is irradiated by 60 MeV protons of cyclotron to generate induced neutrons for ^{188}W and ^{90}Sr production via neutron capture. As the neutron energy reduced, the flux gradually increased towards epithermal range to satisfy (n/2n,γ) reactions. The obtained specific activities at saturation were higher than the reported experimental values because the accumulated epithermal flux and nano-sized specimens influence the outcomes. The beta emitters, which are widely utilized in brachytherapy, appeal an alternative route to locally achieve a rational yield. Therefore, the proposed method via neutron activator may ascertain these broad requirements.

1. Introduction

Radioisotopes are radioactive or unstable materials and spontaneously emit some radiations that can be utilized in various areas of industry and medicine [1–3]. Many of them are generated by bombarding designed targets with neutrons, which are now widely available in nuclear reactors [4–6]. Also, small medical accelerators or cyclotrons can produce the desired radionuclides via high-energy incident particles on a suitable target [7–10]. The effective radiation dose is therapeutically resolved by physical and chemical properties of the radionuclide [11]. Some recent researches have demonstrated that radionuclides with long-range beta emission, like ^{90}Y and ^{188}Re, are the most efficient agents for irradiating of larger tumors [6,12–14]. The fortune of radiotherapy relies not only on the choice of a suitable radionuclide, but also on the pharmacokinetic and pharmacodynamic characteristics of the radiolabeled targeting medium. As currently the most sensitive non-invasive modality for recognizing and outlining biomarkers with different diseases, nuclear medicine and spectroscopy play a strategic role in this development [15–18]. Many of these biomarkers or their disposition ligands may be translated into capable imaging agents. These agents can be employed to detect the attendance of suitable molecular targets if labeled with gamma or beta emitters, or they are also suitable for targeted radiation therapy.

^{188}Re with 17 h half-life, 84% beta with 2.12 MeV maximum energy and 16% gamma at 155 keV is currently of interest for a multitude of therapeutic applications like brachytherapy [6]. Also, its gamma-line at 155 keV enables simultaneous imaging with the usual ^{99m}Tc settings of Single Photon Emission Computed Tomography (SPECT) imaging [19,20]. The ^{188}Re beta emissions have adequate penetration over a maximum range of approximately 10.5 mm for tumor excision involving pericapsular lesions while preventing injury to neighboring normal tissues. By virtue of its short physical half-life and high energy, ^{188}Re suggests the opportunity of depositing more energy in a shorter time than with other radionuclides with longer half-lives [21].

On the other hand, ^{90}Y with 64.1 h half-life, 99.99% β^- with

E-mail addresses: abkhorshidi@yahoo.com, abkhorshidi@chmail.ir.

https://doi.org/10.1016/j.net.2023.02.013

2.28 MeV maximum energy decays to ^{90}Zr with 0.01% gamma at 1.76 MeV [22]. During the decay, the interaction between emitted betas —with 11.3 mm maximum range— and tissue can lead to bremsstrahlung emission. This radiation may be utilized for imaging by SPECT during treatment to discover the seed location and relevant metabolism. ^{90}Y is generally produced by β^- decay of ^{90}Sr, which has a half-life of almost 29 yrs and is a fission product of uranium in nuclear reactors. While the ^{90}Sr decays, the ^{90}Y is isolated in high purity by chemical separation before precipitation [23,24]. ^{90}Y plays an important role in the treatment of lymphoma, leukemia and hepatocellular carcinoma (HCC) [25]. Trans-arterial radioembolization is usually carried out by interventional radiologists, in which micro-spheres impregnated with ^{90}Y are injected into the arteries supplying the tumor. The micro-spheres settled in blood vessels are enclosed the tumor and resulted to damage tumor cells [26,27].

Fundamentally, there are some key factors in the regular production of radioisotopes using nuclear reactors directly or accelerators indirectly. The main issue is to collect an adequate neutron flux to derive a specific neutron interaction. Meanwhile, the target specification and beam quality are the major parameters in order to achieve a reasonable amount of efficacious radiopharmaceuticals. The size of target (in milli-, micro- or nano-scales) besides the irradiation time till 4 to 6 half-lives can drastically affect the saturation yield [3,9,28–32]. Also, the irradiation angle and the target distance from the induced neutron source change the transmutation yield by decelerated neutron capture [11].

In this study, ^{nat}Y(n,γ)Y^{90} reaction is simulated in nano-sized ^{89}Y (stable with 100% abundance) under neutron flux radiation derived from medium-sized research reactor. Also, this nuclear reaction is investigated by induced neutrons from incident 60 MeV protons on a suitable target to simulate the radiation capture in natural yttrium specimens located in a neutron activator. Moreover, ^{186}W(2n,γ)W^{188} reaction is simulated using nano-enriched ^{186}W specimen (stable with 28.6% abundance) which its decay product is ^{188}Re with 99.00% β^- in 0.349 MeV maximum energy range. Here, two different production technologies are investigated for ^{90}Sr/^{90}Y and ^{188}W/^{188}Re generators. Correspondingly, direct and indirect procedures from the research reactor and cyclotron are compared in neutron capture and transmutation of ^{89}Y and ^{186}W specimens by FLUKA simulations.

2. Methods and materials

2.1. Direct production method by research reactor

Nano-sized target materials were defined in FLUKA code as spherical shapes with a radius of 35 nm. They were suspended in 65 nm water thickness like network shape inside a quartz vial with a length of 4 cm and a thickness of 0.1 cm. The specimen-water (S–W) lattice had a uniform distribution in the defined vial, as shown in Fig. 1. The selection of the vial material so that it does not significantly change the neutron flux behavior depends on the physical and chemical characteristics of the target, the heat generation, the irradiation distance and time as well as the specimen size and the activity to be generated [21]. The vial located inside the reactor core was considered under 9E+14 n/cm^2/s neutron flux. The number of particle histories was 1E+8 for the neutron source by an irradiation time of 96 h.

In the simulated reactor spectrum, the fission neutron spectrum derived from the thermal fission of ^{235}U was used from the Goldstein spectrum [33] as follows:

$$\chi\,(E) = 1.75\,\exp\,(-0.766E)\ \mathrm{MeV}^{-1}\ \mathrm{fission}^{-1} \quad (1)$$

Where E is the neutron energy in MeV, and χ (E) is the proportion of the neutrons emitted per energy step per fission. The median energy of a ^{235}U fission neutron is about 2 MeV, which is actually outside the scope of the shape of the spectrum given by Eq. (1).

2.2. Indirect production method by cyclotron

Assorted Nano-sized specimens were simulated by 30 nm radiuses in water as a solution. These specimens were inserted into a three-layer cubic activator of neutrons to achieve an epithermal neutron range derived from a natural tungsten target (^{nat}W) under 60 MeV protons, as shown in Fig. 2. The three neutron activator layers are lead (Pb) moderator enclosed the ^{nat}W target, graphite (C) reflector around the lead cube, and polyethylene absorber surrounds the entire system. The ^{nat}W target was cylindrically shaped under incident 250 μA protons located at the center of the activator to produce induced neutron spectra. The specimen solution was separately laid at 20 and 27 cm distances from the target in the direction of the incident proton beam axis. The S–W solution volume was 2 $\times$ 4 cm^2 area with 2 cm depth inside neutron moderator region. The selected lead moderator slows down the induced fast neutrons speed toward epithermal range by its small mean-free-path. Besides, the graphite reflector was selected to send neutrons back into the moderator region to reach greater neutron flux. The third layer was designed to entrap the escaping neutrons. The transmutation is assessed by yield of production in terms of saturation activity (A_s) during 3 half-lives bombardment, then it is normalized to S–W mass (m), proton beam current (i), and (1-exp [-ln2*$t_{run}/t_{1/2}$]) term, in where t_{run} is running simulation time and $t_{1/2}$ is ^{188}W or ^{90}Y half life. The irradiation time is 3 half-lives of ^{188}Re ($t_{1/2}$ = 17 h) and ^{90}Y ($t_{1/2}$ = 64 h) to attain the saturation yield. The normalized production yield (NPY) in GBq/g per incident proton current is defined as follows:

$$\mathrm{NPY} = [A_s/m/i] *[1\text{-}\exp(\text{-}\ln 2 * t_{run}/t_{1/2})] \quad (2)$$

The previous study [11] has described the changes in thickness of lead and/or water moderators (25, 30, and 35 cm) and graphite reflector (30, 35, and 40 cm) regions to determine the neutron flux behavior. The thicknesses used here in cyclotron-based method have lately been optimized in order to accumulate maximum epithermal neutron flux when deriving the relevant interactions. Also, another survey [9] has compared diverse moderator and reflector materials in determining neutron flux that gathers at different energies.

2.3. Nuclear data library

The interaction cross-section library from TENDL-2019 was used in both simulations to evaluate the production yield [34]. The neutron capture cross-section of ^{186}W(n,γ)W^{187}, ^{187}W(n,γ)W^{188} and ^{89}Y(n,γ)Y^{90} reactions have been compared in Fig. 3 with a Q value of 5.47 eV, 6.83 eV and 6.86 eV, respectively, for the lowest energy state. The maximum cross-section of radiative capture in ^{187}W is in the order of 1E+3 b at epithermal energy range with sparse resonance peaks. For ^{89}Y, this amount is in the order of 1E+1 b at epithermal energy range with wider and more compact resonance peaks. Therefore, in the event of collisions with the moderator nuclei, the neutrons generated should be decelerated from their primary energy to appropriate epithermal energy range.

The selected lead moderator with low lethargy and scattering as well as relatively low energy absorption enables perfect moderation gradually and slowly toward neutron capture within compact resonance peaks. If the neutron is not absorbed in the first peak of the resonance, the moderator again reduces a small amount of

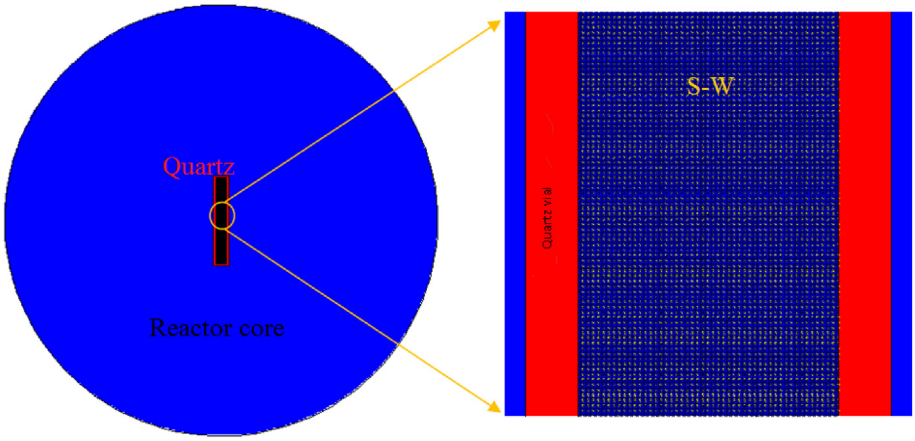

Fig. 1. Quartz vial inside the reactor core which includes segmented nano specimen-water (S–W) solution.

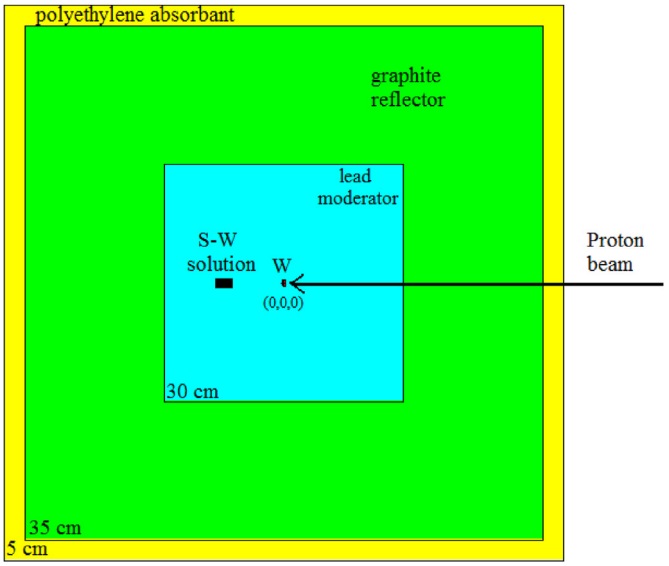

Fig. 2. Specimen-water (S–W) solution inside neutron activator including tungsten target under proton bombardment, lead moderator with 30 cm thickness, 35 cm graphite reflector, and 5 cm absorbent polyethylene.

neutron energy due to the low lethargy. Consequently, the possibility of absorption in the subsequent resonances increases because of dense resonances.

3. Results

3.1. Neutron flux assessment derived from reactor-based method

The obtained neutron flux spectra have been shown in Fig. 4 at very fast ($E_n > 1$ MeV) and epithermal (0.1eV < En < 5 keV) ranges. The differential flux (n/cm^2/s/MeV) in water and quartz regions had an almost similar growing behavior toward low energies. The acquired flux showed greater value at epithermal range by about 1E+26 n/cm^2/s/MeV to satisfy the (2n,γ) and (n,γ) reactions for ^{188}W and ^{90}Y production. Also, the very fast neutron flux was estimated to be about 1E+23 n/cm^2/s/MeV both in the water moderator and in the quartz vial. Respectively, the production yields were 223 and 11100 GBq per gram of ^{186}W and ^{89}Y specimens at saturation according to Table 1. While the water moderator reduced the neutron velocity in the direction of epithermal range, the neutron capture rate for yttrium occurred more than the tungsten specimen. Since the ^{186}W requires two neutrons to capture, its yield is lower. Meanwhile, ^{188}W concentration is reliant upon the short-lived ^{187}W concentration and its decay as well as the radiation time. In comparison with yttrium ($\rho = 4.47$ g/cm^3) production and according to the same irradiation time, tungsten ($\rho = 19.3$ g/cm^3) revealed less production yield due to its density and disintegration or burn-up per gram. Since ^{89}Y has more compact resonance peaks than ^{186}W at epithermal range [34], the yield is greater.

3.2. Production yield evaluation in cyclotron-driven activator

Fig. 5 demonstrates the accumulated neutron flux inside three regions of the simulated activator at total and epithermal ranges of neutron energy. At total energy range, the gathered neutron flux in the graphite region was greater than that of the lead moderator with a huge difference. The flux gradually increased with decreasing neutron energy. At epithermal range, the flux behavior was approximately similar in regions between 1E+14 and 1E+15 n/cm^2/s/MeV. Table 1 shows the predicted production yield for both specimens at two different distances within the moderator region. As the distance increased, the neutron energy steadily decreased within the lead region with a small lethargy. Therefore towards the epithermal energy range, the obtained yield raised at 27 cm from the induced neutron source in the center of the activator. Since the flux showed greater amounts inside the graphite region of the activator, placing specimens inside the reflector region may increase the production yield due to more reduction in neutron energy.

4. Discussion

More importantly, ^{188}Re and ^{90}Y are recently used in radio-synovectomy in patients with chronic hemophilic synovitis, recurrent hemarthrosis, and rheumatoid arthritis to reduce the synovial thickness and effects [35,36]. The mean tissue penetrations of beta particles are 3.6 mm and 3.9 mm for ^{188}Re and ^{90}Y, respectively. Also, their decay by isomer transition is useful for pain relief of bone metastasis besides radio-synovectomy in which the bone marrow and the nearby normal tissues are damaged less. Simultaneously, the emitted gamma photon is also ideal for dosimetry and imaging procedures. Due to the different energies of the beta particles, the intra-articular radiation can be adapted to the size of the joint, whereby the cartilage and the surrounding

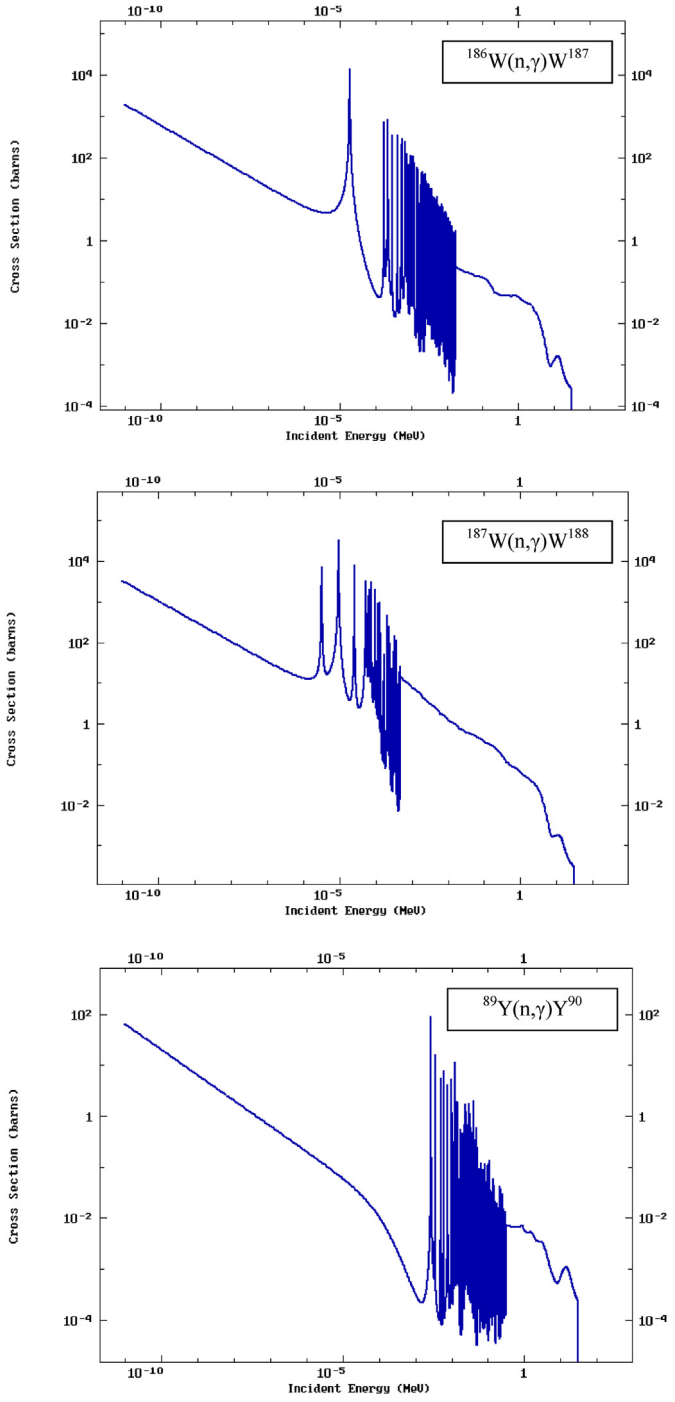

Fig. 3. Neutron capture cross section at epithermal energy range for ^{186}W with resonance peaks by about 1E+2 b, ^{187}W with sporadic peaks by about 1E+3 b, and ^{89}Y with more dense resonance peaks by about 10 b.

structures are protected. The limited availability of these radiopharmaceuticals and their relatively high costs are the main disadvantages for the spread of this form of treatment. Hence, it is important to identify alternative methods that may be manufactured locally or supplied by long life generators.

The selection criteria for radionuclide therapy must include the chemical and physical properties of nano-spheres. The ideal characteristics for radioactively labeled particles or nano-spheres for intra-cavity therapy are: small photo-fraction and intermediate

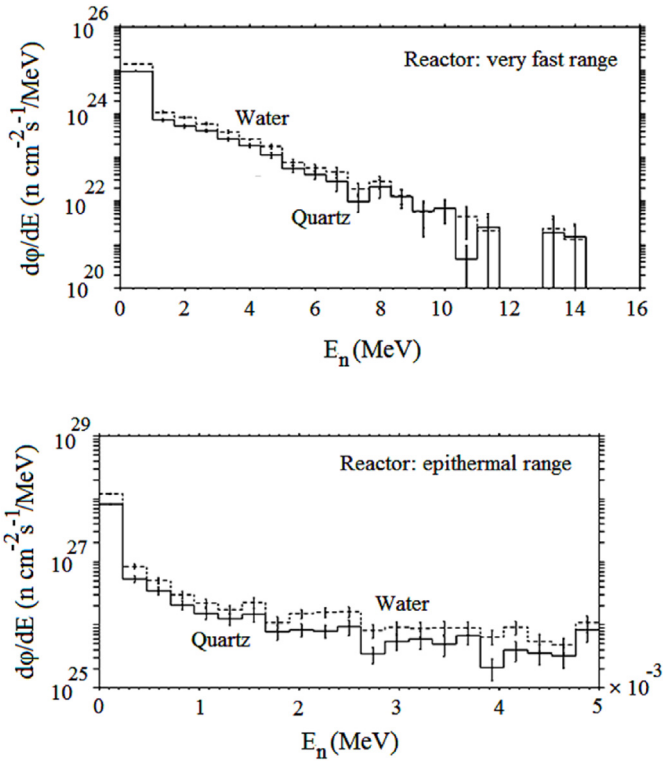

Fig. 4. Neutron flux behavior in water (dash-line) and quartz (solid-line) derived from reactor method for: a) very fast, b) epithermal ranges.

Table 1
Normalized Production yield (GB/g) from neutron capture in reactor and cyclotron methods at saturation.

Method	Reaction	
	$^{186}W(2n,\gamma)W^{188}$	$^{89}Y(n,\gamma)Y^{90}$
Reactor	223	11100
Cyclotron	92 (at 20 cm)	4625 (at 20 cm)
	113 (at 27 cm)	4779 (at 27 cm)

half-life (days), relative simplicity of labeling with high-energy beta particles, high chemical stability to withstand the elution of radioactive markers, high mechanical stability against decomposition, uniform density to avert streaming or settling, uniform size, and removal of macrophage or radiolysis.

^{90}Y can be acquired with a high specific activity (2E+16 Bq/g) by isolating ^{90}Sr from nuclear waste with a very long half-life (about 27 yrs). A number of separation methods have been suggested to isolate ^{90}Y from ^{90}Sr, including extraction chromatography, ion exchange through supported liquid membrane (SLM), solvent extraction, and electrochemical deposition. Each of these techniques has its own disadvantages and advantages in terms of complex configuration and the purity of the end products. On the other hand, there are a number of carrier molecules that can be utilized to advantage in the manufacture of therapeutic radiopharmaceuticals that target various types of cancer. These include small biomolecules, peptides, and antibodies [23]. By greatly small size of <100 nm, nanoparticles present the option of conjugation of binding sites or other targeted units with radionuclides. This property can passively penetrate the tumor and transfer cytotoxic radionuclides with extreme selectivity and minimum side impacts to bind sites within tumor. Two procedures are known for the transfer:

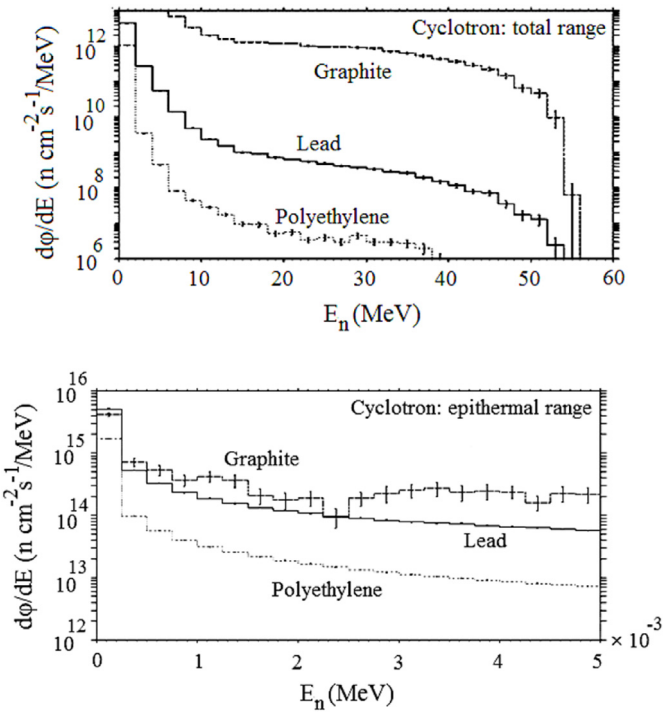

Fig. 5. Neutron flux behavior in three regions of neutron activator derived from cyclotron method for: a) total, b) epithermal ranges.

(a) By passive incorporation specifically for the target tissue
(b) By docking to tumor target structures (receptors, antigens, and/ or angiogenesis sites), in which it is a procedure intervened in targeting units with elevated tumor affinity.

Therapeutically, active radionuclides can be inserted either in or on nanoparticles by encapsulation in the particle or by annexing to existing bind sites on the particle surface. This procedure would principally enable the combination of emitters with diagnostic and therapeutic functions besides implementation in several imaging modalities like PET and SPECT [19,20].

^{90}Y, ^{188}Re, ^{131}I, and ^{67}Cu are radionuclides in passive nano-targeting that can be employed for therapeutic aims via encapsulating in liposome. Attempts have also been made to couple ^{186}Re to liposome via N,N-bis(2-mercaptoethyl) dimethylethylenediamine. Researches on the parallel labeling of liposomes with ^{188}Re and ^{111}In are part of the effort to join therapy with diagnostics (theranostics). In addition, different routes have been attempted to achieve joint delivery of chemotherapeutic agents and radionuclides for diagnosis and treatment using liposomes. Ting et al. [37] give a good overview of efforts to attain multi-modal targeting of tumors by the latest technology using radio-nanoparticles with elevated tumor affinity. The following major examinations provide an adequate depiction of the current state of studies:

(1) Induced Auger radiation, antisense-arbitrated cytotoxicity of tumor cells utilizing a three-component streptavidin release nanoparticle with ^{111}In [38];
(2) Intra-tumoral transfer of a theranostic metallofullerene (f-$Gd_3N@C_{80}$) labeled with ^{177}Lu and DOTA (^{177}Lu DOTA-f-GdN@C), which enables a possible combination of therapy and MRI imaging [39];
(3) Examination and synthesis of the cell uptake of a dual procedure ^{188}Re histidyl-glycyl-arginyl-glycyl-aspartic acid F–CdTe quantum dot probe for joint MRI imaging and therapeutic targeting of angiogenesis [40–42].

Since the ^{90}Y is demanded for preparation of labeled peptides and antibodies that are used for target therapy, the ^{90}Zr(n,p)Y^{90} reaction may be alternatively utilized by a100% enriched ^{90}Zr target under the neutron flux of reactor-based method. This method necessitates a very fast neutron flux of approximately 7.5×10^{13} cm^{-2}s^{-1} [43]. Although this way is perceptibly favorable as a feasible procedure, there are some aspects related to the long-term accessibility and cost of enriched ^{90}Zr. Meanwhile, the need for a very fast neutron flux, the research and development affiliated with the target design and the requirement to separate ^{90}Zr and ^{90}Y recycling are significant problems that need to be addressed [44]. The levels of ^{90}Y activity produced in this way will also be restricted.

^{188}W and ^{90}Y production yield is a function of epithermal neutron flux and irradiation time in high flux reactor or medium cyclotron methods. Dash and Knapp Jr [13] have reported 44.4 GB/g of ^{188}W saturation yield under 6E+14 n/cm^2/s neutron flux of reactor and 40 days irradiation time. Also, Mirzadeh et al. [45] experimentally achieved 8.1 GBq per 183.1 mg of ^{186}W specimen at saturation under 24 days irradiation of 1E+15 n/cm^2/s reactor neutron flux.

In reactor-based method of ^{90}Y production, noticeable levels of ^{89}Sr can be observed as impurity that are formed via (n,p) reaction in corrival. Vimalnath et al. [14] produced ^{90}Y by 851 MBq/mg of Y_2O_3 micro-sized target under 1E+14 n/cm^2/s thermal neutron flux for 14 days irradiation by a medium flux research reactor. However this small specific activity is limited by inadequate epithermal neutron flux, Ponsard [21] has reported 2220 GBq/g of ^{89}Y enriched target by 9 days irradiation in a thermal neutron flux of 3.5E+14 n/cm^2/s. In our study, the average energy of ^{235}U fission neutron is about 2.5 MeV, which is actually outside the scope of the spectrum shaping given by Eq. (1). This is just to highlight that it is the higher energy, more penetrating fission neutrons that are of the utmost importance in reactor shielding submissions. A reactor with high thermal neutron flux (up to 1E+15 n/cm^2/s) and high fast neutron flux (up to 6E+14 n/cm^2/s above 100 keV) is required to generate a suitable production yield of ^{90}Y and ^{188}Re. On the other hand, research reactors such as Tehran reactor in pool-type light water by 2.5E+13 n/cm^2/s neutron flux, which operates with 20% uranium enrichment and has a thermal capacity of 5 MW, do not provide a suitable neutron flux for the production of these radioisotopes [44]. Regarding the shielding issue, there are some materials that are of the utmost importance in the design of the facilities. Of these, lead, steel and concrete have already been addressed in terms of shielding against induced gamma and X-rays [46,47]. In cyclotron-based method, using boron instead of polyethylene can absorb the waste neutrons. According to the neutron activator plan, the reflector region was also designed around the lead region in order to prevent neutron loss. A suitable reflector material should have a high elastic scattering cross-section and a low absorption cross-section so that neutrons can re-enter the moderator region. In the proposed design, graphite with an optimum thickness of 35 cm was chosen as the reflector material in order to maintain the neutrons in a superior flux [2,7,11]. During the cyclotron-based treatment process, the use of collimator and appropriate shielding can reduce the additional dose to the patient along with reducing pollutant production [48]. By injectable or implanting treatment techniques, the patient must be quarantined for a while until the amount of radiation received drops below the non-harmful level [49].

In both methods, filter design with proper material and sufficient thickness can diminish the undesirable dose to the patient. Also, the use of wedge with a suitable attenuator can reduce the

additional dose and induced detrimental effects during the treatment [50,51].

In this study for both radionuclides, the obtained specific activities at saturation were higher than the amounts reported experimentally, because the simulation outcomes are commonly within a factor of 2–4 of experimental ones. Besides, the accumulated epithermal flux and nano-sized target affect the results in the reactor-based method. In addition, an indirect production method based on medium cyclotrons was simulated by a proposed neutron activator in order to evaluate the behavior of the neutron flux and the derived yield as technology accessible to hospitals. An important effect on the production yield is the target thickness, which describes self-shielding impact factor, so that different dimensions of the specimen in micro- and milli-sized target and the type of specification can cause a significant difference in productivity. On the other hand, flux tolerances derived from kind of moderator and reflector materials change the saturation yield at the end of irradiation. Here, the type of material selected with high transparency in relation to the fast neutron for moderator as well as the high reflectivity for reflector can increase the collected neutron flux.

Future work may address the different or hybrid moderators and reflectors in the neutron activator via small cyclotron to achieve a reasonable yield of radionuclide production. In addition, the sources of uncertainty can be explored using diverse nuclear data libraries, physical patterns, the execution of particular models, and the use of pre-stressing techniques.

5. Conclusion

Although no gamma radiation by ^{90}Y makes difficult the dosimetric evaluations, its high-energy beta emission enables local delivery of high doses with lower risk of induced necrosis due to limited tissue penetration. Meanwhile, the availability of a kit formulation process with no mutated radioactive type in the generator leads in the treatment being fractionated or repeated. Since ^{188}Re has shorter half-life in comparison with ^{90}Y, approximately five times more activity is necessary to achieve an equivalent patient dose. On the other hand, the unavailability of the kit formulation process and the limited accessibility of the ^{188}W/^{188}Re generator are disadvantages of the ^{188}Re radionuclide. Alternatively, an indirect method has been suggested here using a compact cyclotron in medium range which may be utilized locally in hospitals with a rational production yield.

Compliance with ethical standards

Conflict of interest statement: The author states that there is no conflict of interest.

Data availability

All data required to support the results and conclusions of the study have been provided here with the submission.

Ethical approval

“Not required”.

Declaration of competing interest

The authors declare that they have no known competing financial interests or personal relationships that could have appeared to influence the work reported in this paper.

References

[1] A. Khorshidi, B. Khosrowpour, S.H. Hosseini, Determination of defect depth in industrial radiography imaging using MCNP code and SuperMC software, Nuclear Engineering and Technology 52 (7) (2020) 1597–1601, https://doi.org/10.1016/j.net.2019.12.010.

[2] A. Khorshidi, Accelerator driven neutron source design via beryllium target and 208Pb moderator for boron neutron capture therapy in alternative treatment strategy by Monte Carlo method, Journal of Cancer Research and Therapeutics 13 (3) (2017) 456–465, https://doi.org/10.4103/0973-1482.179180.

[3] A. Khorshidi, Neutron activator design for 99Mo production yield estimation via lead and water moderators in transmutation's analysis, Instruments and Experimental Techniques 61 (2) (2018) 198–204, https://doi.org/10.1134/s002044121802015x.

[4] M. Jamre, M. Shamsaei, M.G. Maragheh, S. Sadjadi, Novel 175Yb-poly (L-Lactic acid) microspheres for transarterial radioembolization of unrespectable hepatocellular carcinoma, Iran J Pharm Res 18 (2) (2019) 569–578, https://doi.org/10.22037/ijpr.2019.1100668.

[5] A. Khorshidi, Gold nanoparticles production using reactor and cyclotron based methods in assessment of 196,198Au production yields by 197Au neutron absorption for therapeutic purposes, Materials Science and Engineering C 68 (2016) 449–454, https://doi.org/10.1016/j.msec.2016.06.018.

[6] A. Khorshidi, M. Ahmadinejad, S.H. Hosseini, Evaluation of a proposed biodegradable 188Re source for brachytherapy application: a review of dosimetric parameters, Medicine 94 (28) (2015), e1098, https://doi.org/10.1097/md.0000000000001098.

[7] A. Khorshidi, Accelerator-based methods in radio-material 99Mo/99mTc production alternatives by Monte Carlo method: the scientific-expedient considerations in nuclear medicine, Journal of Multiscale Modelling 11 (1) (2020), 1930001, https://doi.org/10.1142/S1756973719300016.

[8] F. Razghandi, R. Izadi, A. Mowlavi, Calculation of the dose of samarium-153-ethylene diamine tetramethylene phosphonate (153Sm-edtmp) as a radiopharmaceutical for pain relief of bone metastasis, Iranian Journal of Medical Physics 12 (4) (2015) 278–283, https://doi.org/10.22038/ijmp.2016.6843.

[9] A. Khorshidi, Molybdenum-99 production via lead and bismuth moderators and milli-structure-98Mo samples by the indirect production technique using the Monte Carlo method, Physics Uspekhi 62 (9) (2019) 931–940, https://doi.org/10.3367/UFNr.2018.09.038441.

[10] A. Khorshidi, A. Pazirandeh, Molybdenum transmutation via 98Mo samples using bismuth/lead neutron moderators, Europhysics Letters 123 (1) (2018), 12001, https://doi.org/10.1209/0295-5075/123/12001.

[11] A. Khorshidi, Radiochemical parameters of molybdenum-99 transmutation in cyclotron-based production method using a neutron activator design for nuclear-medicine aims, Eur Phys J Plus 134 (2019) 249, https://doi.org/10.1140/epjp/i2019-12568-3.

[12] A. Rabiei, M. Shamsaei, H. Yousefnia, S. Zolghadri, A.R. Jalilian, R. Enayati, Development and biological evaluation of 90Y-BPAMD as a novel bone seeking therapeutic Agent, Radiochimica Acta 104 (10) (2016) 727–734, https://doi.org/10.1515/ract-2015-2561.

[13] A. Dasha, FF (Russ) Knapp Jr., An overview of radioisotope separation technologies for development of 188W/188Re radionuclide generators providing 188Re to meet future research and clinical demands, RSC Adv 5 (2015) 39012–39036, https://doi.org/10.1039/C5RA03890A.

[14] K.V. Vimalnath, S. Chakraborty, A. Rajeswari, H.D. Sarma, J. Nuwad, U. Pandey, K. Kamaleshwaran, A. Shinto, A. Dash, Radiochemistry, pre-clinical studies and first clinical investigation of 90Y-labeled hydroxyapatite (HA) particles prepared utilizing 90Y produced by (n,γ) route, Nuclear Medicine and Biology 42 (5) (2015) 455–464, https://doi.org/10.1016/j.nucmedbio.2015.01.006.

[15] A. Khorshidi, Assessment of SPECT images using UHRFB and other low-energy collimators in brain study by Hoffman phantom and manufactured defects, Eur. Phys. J. Plus 135 (2020) 261, https://doi.org/10.1140/epjp/s13360-020-00238-6.

[16] A. Asgari, M. Ashoor, L. Sarkhosh, A. Khorshidi, P. Shokrani, Determination of gamma camera's calibration factors for quantitation of diagnostic radionuclides in simultaneous scattering and attenuation correction, Current Radiopharmaceuticals 12 (1) (2019) 29–39, https://doi.org/10.2174/1874471011666180914095222.

[17] J.S. Nabipour, A. Khorshidi, Spectroscopy and optimizing semiconductor detector data under X and γ photons using image processing technique, Journal of Medical Imaging and Radiation Sciences 49 (2) (2018) 194–200, https://doi.org/10.1016/j.jmir.2018.01.004.

[18] A. Khorshidi, M. Ashoor, S.H. Hosseini, A. Rajaee, Estimation of fan beam and parallel beam parameters in a wire mesh design, Journal of Nuclear Medicine Technology 40 (1) (2012) 37–43, https://doi.org/10.2967/JNMT.111.089904.

[19] A. Takahashi, K. Himuro, S. Baba, Y. Yamashita, M. Sasaki, Comparison of TOF-PET and bremsstrahlung SPECT images of yttrium-90: a Monte Carlo simulation study, Asia Ocean J Nucl Med Biol 6 (1) (2018) 24–31, https://doi.org/10.22038/aojnmb.2017.9673.

[20] M. Ashoor, A. Khorshidi, Evaluation of crystals' morphology on detection efficiency using modern classification criterion and Monte Carlo method in nuclear, Proceedings of the National Academy of Sciences India Section A - Physical Sciences 89 (3) (2019) 579–585, https://doi.org/10.1007/s40010-018-0482-x.

[21] B. Ponsard, Production of radioisotopes in the BR2 high-flux reactor for applications in nuclear medicine and industry, Journal of Labelled Compounds and Radiopharmaceuticals 50 (5-6) (2007) 333–337, https://doi.org/10.1002/jlcr.1377.
[22] H. Poorbaygi, S.M. Aghamiri, S. Sheibani, A. Kamali-asl, E. Mohagheghpoor, Production of glass microspheres comprising 90Y and 177Lu for treating of hepatic tumors with SPECT imaging capabilities, Applied Radiation and Isotopes 69 (10) (2011) 1407–1414, https://doi.org/10.1016/j.apradiso.2011.05.026.
[23] A.R. Jalilian, D. Beiki, A. Hassanzadeh-Rad, A. Eftekharr, P. Geramifar, M. Eftekhari, Production and clinical applications of radiopharmaceuticals and medical radioisotopes in Iran, Seminars in Nuclear Medicine 46 (4) (2016) 340–358, https://doi.org/10.1053/j.semnuclmed.2016.01.006.
[24] A. Vakili, A.R. Jalilian, E. Radfar, A. Bahrami-Samani, S. Shirvani-Arani, B. Salami, M. Ghannadi-Maragheh, Optimization of 90Y-antiCD20 preparation for radioimmunotherapy, Iranian Journal of Nuclear Medicine 18 (1) (2010) 16 (n/a).
[25] D.S. Wang, J.D. Louie, D.Y. Sze, Evidence-based integration of yttrium-90 radioembolization in the contemporary management of hepatic metastases from colorectal cancer, Tech Vasc Interv Radiol 22 (2) (2019) 74–80, https://doi.org/10.1053/j.tvir.2019.02.007.
[26] N. Gholipour, A.R. Jalilian, A. Khalaj, F. Johari-Daha, K. Yavari, O. Sabzevari, A.R. Khanchi, M. Akhlaghi, Preparation and radiolabeling of a lyophilized (kit) formulation of DOTA-rituximab with 90Y and 111In for domestic radioimmunotherapy and radioscintigraphy of Non-Hodgkin's Lymphoma, DARU Journal of Pharmaceutical Sciences 22 (2014) 58, https://doi.org/10.1186/2008-2231-22-58.
[27] M.R. Ghahramani, A.A. Garibov, T.N. Agayev, M.A. Mohammadi, A novel way to production yttrium glass microspheres for medical applications, Glass Physics and Chemistry 40 (3) (2014) 283–287, https://doi.org/10.1134/S1087659614030055.
[28] S.J. Wang, W.Y. Lin, M.N. Chen, B.T. Hsieh, L.H. Shen, Z.T. Tsai, G. Ting, J.T. Chen, W.L. Ho, S. Mirzadeh, F.F. Knapp Jr., Rhenium-188 microspheres: a new radiation synovectomy agent, Nuclear Medicine Communications 19 (5) (1998) 427–433, https://doi.org/10.1097/00006231-199805000-00004.
[29] C. Bouvry, X. Palard, J. Edeline, V. Ardisson, P. Loyer, E. Garin, et al., Transarterial radioembolisation (TARE) agents beyond 90Y-microspheres, Biomed Res Int 2018 (2018), 1435302, https://doi.org/10.1155/2018/1435302.
[30] E. Verger, P. Drion, G. Meffre, C. Bernard, L. Duwez, N. Lepareur, et al., 68Ga and 188Re starch-based microparticles as theranostic tool for the hepatocellular carcinoma: radiolabeling and preliminary in vivo rat studies, PLoS ONE 11 (2016), e0164626, https://doi.org/10.1371/journal.pone.0164626.
[31] A. Cikankowitz, A. Clavreul, C. Tétaud, L. Lemaire, A. Rousseau, N. Lepareur, et al., Characterization of the distribution, retention, and efficacy of internal radiation of 188Re-lipid nanocapsules in an immunocompromised human glioblastoma model, J Neurooncol 131 (2017) 49–58, https://doi.org/10.1007/s11060-016-2289-4.
[32] B.A. Hrycushko, A.N. Gutierrez, B. Goins, W. Yan, W.T. Phillips, P.M. Otto, et al., Radiobiological characterization of post-lumpectomy focal brachytherapy with lipid nanoparticle-carried radionuclides, Phys Med Biol 56 (2011) 703–719, https://doi.org/10.1088/0031-9155/56/3/011.
[33] J. Wood, Computational Methods in Reactor Shielding, Chapter 3 - RADIATION SOURCES, Elsevier, 1982, pp. 56–78, https://doi.org/10.1016/B978-0-08-028685-3.50006-X. Available online 2013;.
[34] ENDF-6, Evaluated Nuclear Data File (ENDF), TENDL, 2019. https://www-nds.iaea.org/exfor/endf.htm.
[35] A.R. Kachooei, A. Heidari, G. Divband, M.E. Zandinezhad, A. Mousavian, H. Farhangi, B. Aminzadeh, A. Zarifian, F. Bagheri, Z. Badiei, Rhenium-188 radiosynovectomy for chronic haemophilic synovitis: evaluation of its safety and efficacy in haemophilic patients, Haemophilia 26 (1) (2020) 142–150, https://doi.org/10.1111/hae.13880.
[36] K. Liepe, J.J. Zaknun, A. Padhy, E. Barrenechea, V. Soroa, S. Shrikant, P. Asavatanabodee, M.J. Jeong, M. Dondi, Radiosynovectomy using yttrium-90, phosphorus-32 or rhenium-188 radiocolloids versus corticoid instillation for rheumatoid arthritis of the knee, Annals of Nuclear Medicine 25 (2011) 317–323, https://doi.org/10.1007/s12149-011-0467-1.
[37] G. Ting, C. Chang, H. Wang, T. Lee, Nanotargeted radionuclides for cancer nuclear imaging and internal radiotherapy, J. Biomed. Biotechnol. (2010), 953537, https://doi.org/10.1155/2010/953537.
[38] X. Liu, Y. Wang, K. Nakamura, s Kawauchi, A. Akalin, D. Cheng, L. Chen, M. Rusckowski, D.J. Hnatowich, Auger radiation-induced, antisense-mediated cytotoxicity of tumor cells using a 3-component streptavidin-delivery nanoparticle with 111In, J. Nucl. Med. 50 (4) (2009) 582–590, https://doi.org/10.2967/jnumed.108.056366.
[39] J.W. Bulte, Science to practice: can theranostic fullerenes be used to treat brain tumors? Radiology 261 (1) (2011) 1–2, https://doi.org/10.1148/radiol.11111636.
[40] Z. Li, G. Zhang, H. Shen, L. Zhang, Y. Wang, Synthesis and cell uptake of a novel dual modality 188Re-HGRGD (D) F-CdTe QDs probe, Talanta 85 (2) (2011) 936–942, https://doi.org/10.1016/j.talanta.2011.04.077.
[41] M. Ashoor, A. Khorshidi, A. Pirouzi, A. Abdollahi, M. Mohsenzadeh, S.M.Z. Barzi, Estimation of Reynolds number on microvasculature capillary bed using diffusion and perfusion MRI: the theoretical and experimental investigations, Eur. Phys. J. Plus 136 (2021) 152, https://doi.org/10.1140/epjp/s13360-021-01145-0.
[42] M. Ashoor, A. Khorshidi, L. Sarkhosh, Estimation of microvascular capillary physical parameters using MRI assuming a pseudo liquid drop as model of fluid exchange on the cellular level, Rep Pract Oncol Radiother 24 (1) (2019) 3–11, https://doi.org/10.1016/j.rpor.2018.09.007.
[43] I.A. Abbasi, J.H. Zaidi, M. Arif, S. Waheed, M.S. Subhani, Measurement of fission neutron spectrum averaged cross sections of some threshold reactions on zirconium: production possibility of no-carrier-added 90Y in a nuclear reactor, Radiochim Acta 94 (8) (2006) 381–384, https://doi.org/10.1524/ract.2006.94.8.381.
[44] N. Zare, G. Jahanfarnia, A. Khorshidi, J. Soltani, Robustness of optimized FPID controller against uncertainty and disturbance by fractional nonlinear model for research nuclear reactor, Nuclear Engineering and Technology (2020), https://doi.org/10.1016/j.net.2020.03.002. In press.
[45] S. Mirzadeh, M. Du, A. Beets, F.F. Knapp, Russ). Thermoseparation of neutron-irradiated tungsten from Re and Os, Ind Eng Chem Res 39 (9) (2000) 3169–3172, https://doi.org/10.1021/ie990582x.
[46] M. Ashoor, A. Khorshidi, L. Sarkhosh, Appraisal of new density coefficient on integrated-nanoparticles concrete in nuclear protection, Kerntechnik 85 (1) (2020) 9–14, https://doi.org/10.3139/124.190016.
[47] A. Khorshidi, A. Abdollahi, A. Pirouzi, S.H. Hosseini, Band pass filter plan in fluoroscopy for high energy range, SN Appl. Sci. 2 (2020) 90, https://doi.org/10.1007/s42452-019-1885-2.
[48] M. Rabiei, A. Khorshidi, J. Soltani-Nabipour, Production of Yttrium-86 radioisotope using genetic algorithm and neural network, Biomedical Signal Processing and Control 66 (2021), 102449, https://doi.org/10.1016/j.bspc.2021.102449.
[49] S. Salari, A. Khorshidi, J. Soltani-Nabipour, Simulation and assessment of 99mTc absorbed dose into internal organs from cardiac perfusion scan, Nuclear Engineering and Technology 55 (1) (2023) 248–253, https://doi.org/10.1016/j.net.2022.08.024.
[50] H. Imani-Shirvanehdeh, A. Khorshidi, J. Soltani-Nabipour, A. Alipour, K. Arbabi, Design and construction of a cylindrical ionization chamber for reference dosimetry in radiation protection, Iran J Sci Technol Trans Sci 45 (2021) 1837–1841, https://doi.org/10.1007/s40995-021-01153-w.
[51] M. Ashoor, A. Khorshidi, Point-spread-function enhancement via designing new configuration of collimator in nuclear medicine, Radiation Physics and Chemistry 190 (2022), 109783, https://doi.org/10.1016/j.radphyschem.2021.109783.